Chemical Vapor Deposition

DOI: 10.1002/cvde.200500023

Review

MOCVD and ALD of High-κ Dielectric Oxides Using Alkoxide Precursors**

By *Anthony C. Jones,* Helen C. Aspinall, Paul R. Chalker, Richard J. Potter, Troy D. Manning, Yim Fun Loo, Ruairi O'Kane, Jeffrey M. Gaskell,* and *Lesley M. Smith*

A number of high-permittivity (κ) dielectric oxides are currently being investigated as alternatives to SiO_2 as the dielectric insulating layer in sub-0.1 μm CMOS technology. Metal-organic (MO)CVD and atomic layer deposition (ALD) are promising techniques for the deposition of these high-κ dielectric oxides. In this paper it is shown how the use of "designed" metal alkoxide precursors, containing bidentate donor-functionalized alkoxide ligands, in MOCVD leads to a marked improvement in the physical properties of the MOCVD precursors and process parameters. However, the use of such ligands is not as beneficial in the ALD process, highlighting the very different requirements of MOCVD and ALD precursors.

Keywords: Hafnium aluminate, Hafnium oxide, Lanthanide oxides, Metal alkoxide precursors, Zirconium oxide.

1. Introduction

The demand for smaller, faster transistors in computer processors and other silicon ICs has driven the continuous reduction (or "scaling") in the dimensions of metal-oxide-semiconductor field-effect transistors (MOSFETs). This scaling has forced a rapid decrease in both the channel length and SiO_2 gate dielectric thickness.[1] However, as the gate thickness approaches 2–3 nm, direct electron tunneling and high leakage currents present serious obstacles to future device reliability.[2] These problems can be overcome by replacing the SiO_2 ($\kappa \sim 3.9$) with a higher dielectric constant (κ) material, allowing an equivalent capacitance to be achieved using a physically thicker insulating layer. Consequently there has been much recent research into alternative high-κ dielectric oxides or silicates,[2] such as Al_2O_3,[3] ZrO_2,[4] HfO_2,[5] Zr and Hf silicate,[6,7] $(HfO_2)_x(Al_2O_3)_{1-x}$,[8,9] La_2O_3,[10] Pr_2O_3,[11] Y_2O_3,[12] Gd_2O_3,[12,13] and Nd_2O_3.[14] High-κ materials also have significant potential as replacements for SiO_2 or Si_3N_4 in the storage capacitors of dynamic random access memory (DRAM) devices, and HfO_2/Al_2O_3 nanolaminates are currently under investigation.[15]

A variety of techniques has been used for the deposition of metal oxide films including, physical vapor deposition (radio frequency and magnetron sputtering, ion-beam sputtering, molecular-beam epitaxy, laser ablation),[16–19] solution deposition (sol–gel, metal-organic decomposition),[20,21] MOCVD[22–26] and ALD.[27] Of these techniques, MOCVD and ALD are particularly well suited to modern manufacturing methods for microelectronics.

MOCVD offers the potential for large-area growth, and has the advantages of good composition control, high film uniformity, good doping control, and gives excellent conformal step coverage on nonplanar device geometries. An essential requirement for a successful MOCVD process is the availability of precursors with the appropriate physical properties and decomposition characteristics. The precursor must have an adequate volatility for efficient vapor-phase transport and should deposit high-purity films. There must be an adequate temperature window between precursor evaporation and decomposition, and for many electronics applications the oxide deposition temperature is re-

[*] Prof. A. C. Jones, Dr. H. C. Aspinall, Dr. T. D. Manning, Dr. Y. F. Loo, R. O'Kane, J. M. Gaskell
Department of Chemistry, University of Liverpool
Liverpool, L69 3ZD (UK)
E-mail: tjconsultancy@btconnect.com
Prof. P. R. Chalker, Dr. R. J. Potter
Department of Materials Science and Engineering,
University of Liverpool
Liverpool, L69 3BX (UK)
Dr. L. M. Smith
Epichem Oxides and Nitrides
Power Road, Bromborough, Wirral, Merseyside, CH62 3QF (UK)

[**] We are grateful to the EPSRC and Epichem Limited for support of this work. We are also grateful to Prof. M. Ritala, Dr. K. Kukli, Dr. R. Matero and Prof. M. Leskelä (University of Helsinki, Finland) for many useful discussions on ALD.

stricted, to ~500 °C, so precursors with limited thermal stability are often required. It is also an advantage if the precursor is unreactive to water, giving it a good ambient stability and long shelf-life.

Due to the low vapor pressure and relatively low thermal stability of many oxide precursors, liquid-injection MOCVD is now widely used for the deposition of metal oxide films.[26] In liquid-injection MOCVD the precursor is dissolved in an inert solvent, usually a hydrocarbon (e.g., toluene, heptane, nonane) or an ether (e.g., tetrahydrofuran). The precursor solution is held at room temperature until used in the MOCVD process, preventing thermal decomposition of the precursor. Precursors used in liquid-injection MOCVD must be soluble and stable for long periods in the chosen solvent, and must not react with other precursors in the same solution. In addition, the presence of a single heated evaporator at a fixed temperature makes it important that co-precursors evaporate at a similar temperature, otherwise it will be difficult to control the composition of complex oxides. To optimize the compositional uniformity it is also important that the various precursors deposit oxide in a similar temperature regime.

ALD is a modification of MOCVD,[27] in which gaseous precursors are successively introduced to the substrate surface in a repeated cycle. Between cycles, the volatile reaction products are flushed from the reactor by purging with an inert gas, or evacuation. An ideal ALD process has a self-limiting mechanism in which the growth surface becomes saturated with precursor or reactant molecules, so that film growth automatically stops (or "self-limits") at one or sometimes two monolayers. Under these conditions the film growth rate (nm per cycle) is independent of the precursor pulse length.

ALD relies on surface exchange reactions between chemisorbed metal-containing precursor fragments and adsorbed nucleophilic reactant molecules, such as surface [OH] species. The surface-controlled growth in ALD leads to highly uniform coverage (or conformality) of planar substrates, as well as nonplanar surfaces containing trenches or vias, and high surface area (high-aspect-ratio geometries) substrates such as silica and alumina powders.[27] Precursors with the appropriate physical properties and suitable deposition chemistry are therefore essential for the successful ALD of metal oxides. In common with MOCVD precursors, an ALD precursor must be volatile and have an adequate temperature window between evaporation and decomposition. However, in marked contrast to a MOCVD precursor, an ALD precursor should have a relatively high thermal stability so that surface exchange reactions predominate over thermal decomposition, otherwise there will be a breakdown in self-limiting growth. Unlike an "ideal" MOCVD precursor, the ALD precursor must be highly reactive towards nucleophiles such as [OH] otherwise ALD growth rates will be severely inhibited.

Although some existing precursors satisfy the requirements for liquid-injection MOCVD and ALD processes, the rapid growth in the number and complexity of metal oxides deposited by these techniques is making it increasingly necessary to "tailor" the physical properties of a precursor to optimize its physical properties and deposition characteristics.

In this paper, some recent developments in the molecular design of metal alkoxide precursors used for the MOCVD and ALD of a range of high-κ dielectric oxides are described. The influence of molecular structure on the physical properties of a precursor, and on the growth dynamics of the MOCVD and ALD processes are outlined, together with a brief discussion on the material properties and electrical characteristics of the metal oxide films.

2. MOCVD of Dielectric Oxides

2.1. MOCVD of ZrO_2 and HfO_2

ZrO_2 and HfO_2 have high permittivities, with κ values of approximately 25, compared with 3.9 for SiO_2, and are relatively thermodynamically stable in contact with silicon, making them promising alternative high-κ materials.[2] However, the MOCVD of ZrO_2 and HfO_2 has been hindered by problems associated with existing Zr and Hf oxide precursors. For instance, $ZrCl_4$[28] and $HfCl_4$[29] are low-volatility solids which need substrate temperatures of 800 °C and above for oxide deposition, and there is the possibility

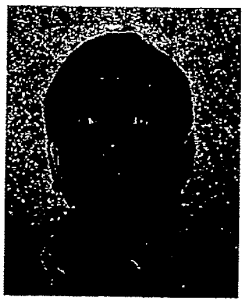

Tony Jones is a Professor in the Department of Chemistry in the University of Liverpool, and Chief Scientist of Epichem Limited. He has over 25 years' experience in the development of precursors for the deposition of compound semiconductors, metal oxides, and metals by metal-organic chemical vapor deposition (MOCVD) and atomic layer deposition (ALD). In 1983 he helped found Epichem Ltd., a major worldwide supplier of MOCVD and ALD precursors.

of chloride contamination in the films. The β-diketonates, $[Zr(acac)_4]$ and $[Hf(acac)_4]$ (acac = pentane-2,4-dionate) require high evaporation temperatures (~200 °C) for sufficient vaporization,[30] and the oxide films are often heavily contaminated with carbon.[31] The β-diketonate $[Zr(thd)_4]$ (thd = 2,2,6,6-tetramethylheptane-3,5-dionate) has been successfully used for the MOCVD of high-purity ZrO_2,[31,32] although it is also relatively involatile and requires high substrate temperatures (>600 °C) for oxide growth. The fluorinated complexes $[Zr(tfac)_4]$ and $[Hf(tfac)_4]$ (tfac = 1,1,1-trifluoropentane-2,4-dionate) are more volatile,[33] but the presence of fluorine, which can react adversely with the Si substrate, is highly undesirable. Recently, two new β-diketonate complexes, $Zr(tod)_4$, and $Hf(tod)_4$ (tod = 2,7,7-trimethyl-3,5-octanedionate) have been used to deposit ZrO_2 and HfO_2 by liquid-injection MOCVD. The complexes were found to give higher oxide growth rates at lower deposition temperatures than the corresponding thd complexes.[34]

The metal nitrate complexes $[Zr(NO_3)_4]$ and $[Hf(NO_3)_4]$ have been used for the MOCVD of high-purity ZrO_2 and HfO_2 films at growth temperatures as low as 300 °C,[35] but there may be safety concerns about the widespread use of anhydrous nitrate complexes in MOCVD processes. Metal alkylamide complexes have considerable potential as MOCVD precursors for the deposition of both metal nitride and metal oxide thin films. It was shown some time ago that $[Zr(NEt_2)_4]$ can be used for the MOCVD of high quality ZrO_2 films in the temperature range 500–580 °C,[36] and more recently the liquid alkylamide $[Hf(NEt_2)_4]$ has been used to deposit HfO_2 by conventional (i.e., "bubbler-based") MOCVD.[37,38]

Metal alkoxides are attractive MOCVD precursors as they permit lower deposition temperatures and, under optimum growth conditions, allow the deposition of carbon-free films.[39] However, the majority of $[Zr(OR)_4]$ and $[Hf(OR)_4]$ complexes are dimeric or polymeric with limited volatility, due to the tendency of the Zr^{IV} and Hf^{IV} atoms to expand their coordination sphere to six, seven, or eight.[40] Metal alkoxide polymerization can be inhibited by the presence of bulky groups such as *tert*-butoxide, and $[Zr(O^tBu)_4]$ and $[Hf(O^tBu)_4]$ are volatile monomeric complexes that have been successfully used for the MOCVD of ZrO_2[41–43] and HfO_2.[44] However, these precursors contain unsaturated, four-coordinate metal centers, and the *tert*-butoxide ligand undergoes a catalytic "hydrolytic thermal decomposition"[45] making them highly air- and moisture-sensitive, and susceptible to pre-reaction in the MOCVD reactor. Consequently, their reactivity leads to a greatly reduced shelf life, especially in solution-based liquid-injection MOCVD applications.

One strategy used to limit oligomerization in Zr and Hf alkoxides is to satisfy the coordination sphere of the central metal atom by introducing bidentate, chelating β-diketonates such as [thd], β-ketoesters (*tert*-butyl acetoacetate, "tbaoac"), or β-ketoamides (*N,N*-diethylacetoacetamide, "deacam"). These heteroleptic complexes potentially combine the advantages of the good ambient stability, associated with metal β-diketonates, with the lower thermal stability and higher volatility of metal alkoxides. The complex, $[Zr_2(OPr^i)_6(thd)_2]$, is a centrosymmetric dimer containing terminal [thd] groups and two bridging $[O^iPr]$ ligands, and has been used for the liquid-injection MOCVD of ZrO_2 over the temperature range 300–600 °C. The films contained 2–11 at.-% of carbon.[46] The complexes $[Zr(O^iPr)_2(tbaoac)_2]$ and $[Zr(O^iPr)_2(deacam)_2]$ are monomeric, and $[Zr(O^iPr)_2(tbaoac)_2]$ has been used for the MOCVD of ZrO_2 in the absence of an added oxidant.[47]

Another strategy for inhibiting the polymerization of metal alkoxides and reducing their moisture sensitivity is to increase the coordination number of the central metal atom by incorporating bidentate donor-functionalized alkoxide ligands into the complex. The sterically-hindered ligand 1-methoxy-2-methyl-2-propanolate, $OCMe_2CH_2OMe$ [mmp], contains two [Me] groups on the α-carbon atom close to the metal center, and can also form stable, bidentate chelate rings with the metal center (Fig. 1). This inhibits the interaction between the metal center and alkoxide ligands of other $M(OR)_4$ molecules, and facilitates the formation of mononuclear metal alkoxide complexes.[48] We have used the [mmp] ligand to prepare a series of complexes, $[Zr(O^tBu)_2(mmp)_2]$, $[Hf(O^tBu)_2(mmp)_2]$, $[Zr(mmp)_4]$, and $[Hf(mmp)_4]$, that are six-coordinate, octahedral monomers in the solid state.[49,50] The crystal structure of $[Hf(mmp)_4]$ (Fig. 2) shows that the complex is a six-coordinate monomer with a distorted octahedral configuration, containing two bidentate [mmp] ligands and two monodentate [mmp] ligands.[50] The increased ligand saturation around the metal centers makes these volatile complexes significantly less reactive to air and moisture than $[M(O^tBu)_4]$ and $[M(NR_2)_4]$ complexes.

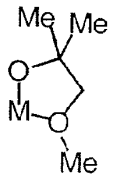

Fig. 1. Chelate ring formed by an [mmp] ligand coordinated to a Group IVB metal.

These $[M(O^tBu)_2(mmp)_2]$ and $[M(mmp)_4]$ (M = Zr, Hf) complexes were used for the liquid-injection MOCVD of ZrO_2 and HfO_2 thin films over the temperature range 350–650 °C.[50] High-frequency capacitance-voltage (*C-V*) measurements on $[Al/MO_2/p\text{-}Si]$ capacitors containing ZrO_2 and HfO_2 layers grown from the $[M(O^tBu)_2(mmp)_2]$ and $[M(mmp)_4]$ precursors showed that the films had good dielectric properties with clear accumulation, depletion,

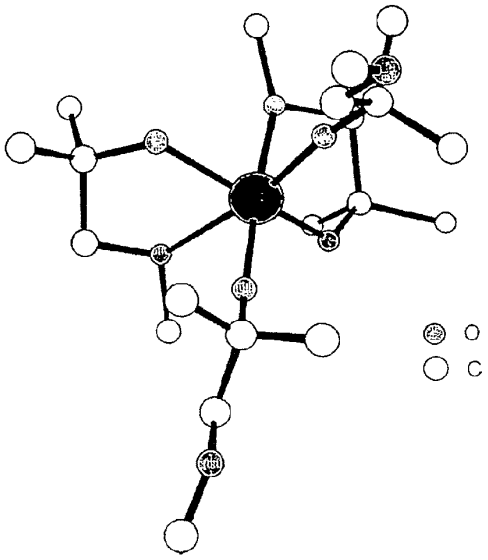

Fig. 2. Crystal structure of [Hf(mmp)$_4$].

and inversion conditions, with only a very small shift in flat-band voltage (ΔV_{FB}) and minimal clockwise hysteresis due to the presence of a small amount of mobile, positively charged ions in the films.[51]

Based on GC-MS studies a mechanism has been proposed for the decomposition of [Hf(mmp)$_4$] in the absence of oxygen (Reaction 1).[52]

$$[Hf(mmp)_4] \rightarrow Hf(OH)_4 + 4(CH_3)_2C{=}CHOCH_3$$
$$[Hf(mmp)_4] \rightarrow HfO_2 + 2[mmpH] + 2(CH_3)_2C{=}CHOCH_3 \quad (1)$$

The main features of the mechanism are the elimination of a β-hydride from [mmp] to form Hf(OH)$_4$ and liberate the alkene $(CH_3)_2C{=}CHOCH_3$, and the transfer of a hydrogen atom to an adjacent [mmp] ligand, both of which facilitate the clean elimination of the mmp ligand.

The donor-functionalized ligand 2-(4,4-dimethyloxazolinyl)-propanolate, ("dmop"), (see Fig. 3) has potential advantages over other donor-functionalized alkoxide ligands in stabilizing large, positively charged metal centers and promoting the formation of volatile monomeric complexes. Instead of forming stable, chelate rings, ligands such as [$OCR_2CH_2NMe_2$] and [OCR_2CH_2OMe] often dangle in the monodentate mode, as in [M(mmp)$_4$] complexes,[50] or bridge metal centers to form dimers, as in the case of [Zr(O^{t}Bu)$_2$(OCH$_2$CH$_2$NMe$_2$)$_2$],[53] [Zr(O^{i}Pr)$_2$(OCH(Me)CH$_2$NMe$_2$)$_2$]$_2$,[54] and [Zr(O^{i}Pr)$_2$-(OCH(CH$_2$NMe$_2$)$_2$)$_2$]$_2$.[54] In the case of [mmp], a facile

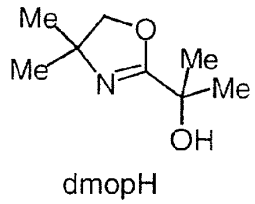

dmopH

Fig. 3. Schematic diagram of the dmopH ligand.

rotation about the C$^\alpha$-C$^\beta$ bond results in conversion from the chelating to monodentate dangling coordination mode (see Fig. 4a). The ligands [$OCH_2CH_2NMe_2$] and [$OCH(Me)CH_2NMe_2$] will also undergo similar facile C$^\alpha$-C$^\beta$ bond rotations, leading to bridging between the metal centers. In contrast, the analogous C$^\alpha$-C$^\beta$ bond rotation

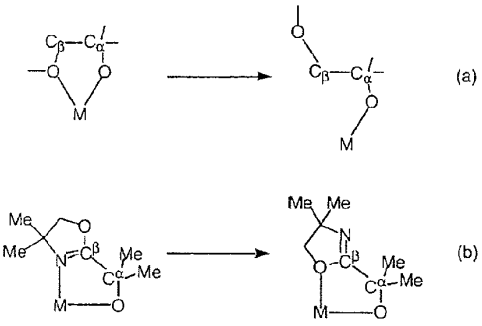

Fig. 4. Possible stereochemical configurations of (a) mmp ligand and (b) dmop ligand. Reproduced with permission from [55]; copyright 2005, Royal Society of Chemistry.

of the N-bonded dmop ligand brings the oxazoline oxygen atom into a suitable position for chelation, as shown in Figure 4b, maintaining a stable, chelating configuration that shields the metal center effectively and inhibits the oligomerization of metal-dmop complexes. This makes [dmop] potentially more effective than other donor-functionalized ligands in promoting monomer formation in a wide range of metal alkoxides.

We have recently synthesized the complexes [M(O^{t}Bu)$_2$(dmop)$_2$] (M = Hf, Zr), and the crystal structure of [Hf(O^{t}Bu)$_2$(dmop)$_2$] is shown in Figure 5. The isomorphous complexes are six-coordinate monomers with a distorted octahedral arrangement of four oxygen and two nitrogen atoms around the central Hf or Zr atom. The complexes contain two *tert*-butoxide groups and two chelating [dmop] groups. The M-O(*t*Bu) σ bond lengths are shorter than the M-O(dmop) σ bonds, and the weaker dative M-N bonds are the longest in the molecule.[55]

Chemical Vapor Deposition

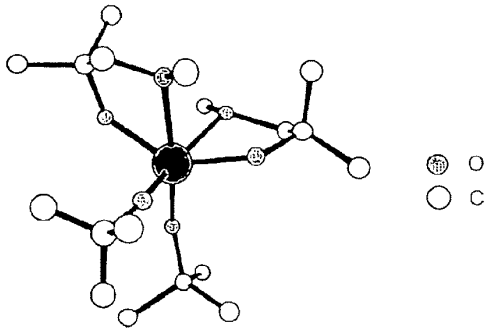

Fig. 5. Crystal structure of $[Hf(O^tBu)_2(dmop)_2]$.

The $[M(O^tBu)_2(dmop)_2]$ complexes are significantly more stable to air and moisture than the $[Hf(O^tBu)_4]$ and $[Zr(O^tBu)_4]$ parent alkoxides, and they are also much less air sensitive than the alkylamide complexes $[Zr(NR_2)_4]$ and $[Hf(NR_2)_4]$. This increased ambient stability makes both complexes very suitable for solution-based liquid-injection MOCVD.[55] Oxide deposition was performed over a wide range of substrate temperatures, from 350 to 550 °C. The ZrO_2 films contained residual carbon at levels of 3.4–5.3 at.-%, whilst the carbon levels in the HfO_2 film varied between 1.9 and 8 at.-%. Analysis by X-ray diffraction (XRD) showed that the films were deposited in the thermodynamically stable *a*- or monoclinic phase.

High-frequency *C-V* measurements were carried out on $[Al/MO_2/n\text{-}Si]$ capacitor structures to measure the dielectric properties of the ZrO_2 and HfO_2 films (see Figs. 6 and 7).[55] Accumulation, depletion, and inversion regions are clearly seen in both cases, typical of good quality dielectric films. The ZrO_2 film showed a relatively small hysteresis between the voltage sweeps, in the forward and reverse directions, of approx. 0.05V, with a flat-band voltage shift of 0.2V. The hysteresis of 0.1V in the HfO_2 film was slightly larger than in the ZrO_2 film, and there is also a larger shift in the flat-band voltage (–1V), indicative of more trapped charge at the MO_2/Si interface. The clockwise hysteresis observed in the *C-V* data of films arises from electron trapping in electronic states at the Si/MO_2 interface and/or in the bulk of the dielectric oxide film. The permittivity values (κ) of the ZrO_2 and HfO_2 films were 21.3 and 18.6, respectively. The reduction from the expected value for each film of $\kappa \sim 25$[2] can be attributed to the series resistance of the Si substrate, and the presence of a low permittivity mixed layer of metal (Zr or Hf) oxide and native SiO_2 ($\kappa = 3.9$) on the non-etched Si substrates.

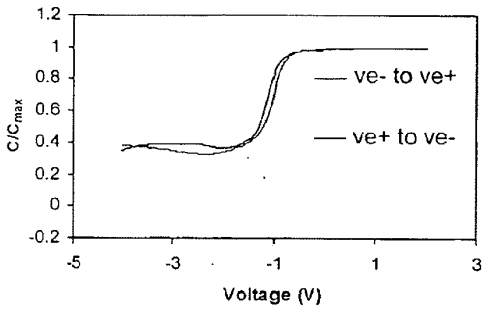

Fig. 7. High frequency *C-V* data for a $[Al/HfO_2/n\text{-}Si]$ capacitor structure grown by liquid-injection MOCVD using $[Hf(O^tBu)_2(dmop)_2]$ (HfO_2 growth temperature = 450 °C). Reproduced with permission from [55]; copyright 2005, Royal Society of Chemistry.

The homoleptic alkoxide $[Hf(dmop)_4]$ is a six-coordinate monomeric complex, containing two bidentate, chelating, dmop ligands and two monodentate, dmop ligands, giving a distorted octahedral arrangement of four oxygen and two nitrogen atoms around the Hf atom, see Figure 8. The Hf-O(dmop) σ bonds are significantly shorter than the weaker

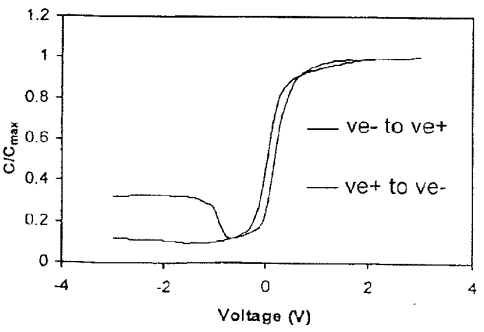

Fig. 6. High-frequency *C-V* data for a $[Al/ZrO_2/n\text{-}Si]$ capacitor structure grown by liquid-injection MOCVD using $[Zr(O^tBu)_2(dmop)_2]$ (ZrO_2 growth temperature = 450 °C). Reproduced with permission from [55]; copyright 2005, Royal Society of Chemistry.

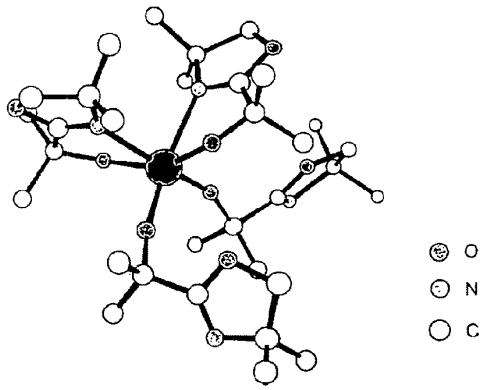

Fig. 8. Crystal structure of $[Hf(dmop)_4]$.

dative Hf-N bonds. [Hf(dmop)$_4$] is significantly less reactive to air and moisture than alkoxides such as [Hf(O^{t}Bu)$_4$] and the alkylamides [Hf(NR$_2$)$_4$], and has also been used successfully for the deposition of HfO_2 films by liquid-injection MOCVD.[56] The films were deposited in the temperature range 350–650 °C. Auger electron spectroscopy (AES) showed that residual carbon (2.1–11.6 at.-%) and nitrogen (0.4–1.9 at.-%) were present in the films. Analysis by XRD showed that the films were amorphous at substrate temperatures < 400 °C, and adopted the monoclinic (α-HfO_2) phase above 450 °C. The C-V data for a [Al/HfO_2/n-Si] capacitor structure demonstrated anticlockwise hysteresis, and a flat-band voltage shift of –0.4V.

2.2. MOCVD of Hf Aluminate

Another approach to stabilizing the Si-HfO_2 interface is to alloy HfO_2 with Al_2O_3, to form hafnium aluminate, $(HfO_2)_x(Al_2O_3)_{1-x}$, which is amorphous up to very high processing temperatures (e.g., 900 °C for Al concentrations of 31 %), and has been reported to retain a relatively high dielectric constant of $\kappa \sim 15$.[8] Although Hf aluminate has been deposited by ALD, using the precursor combinations [$HfCl_4$]/[$AlMe_3$]/H_2O[57,58] and [Hf(NMeEt)$_4$]/[$AlMe_3$]/H_2O,[15] there had been no MOCVD studies until the recent report on the deposition of $(HfO_2)_x(Al_2O_3)_{1-x}$ (Al = 8.4–38.5 at.-%) by liquid-injection MOCVD using the metal alkoxide precursors [Hf(mmp)$_4$] and [Al(OPr^i)$_3$].[59]

The atomic composition of the $(HfO_2)_x(Al_2O_3)_{1-x}$ films was determined by AES, and this showed that the films were all high purity, with no carbon detected (estimated AES detection limit ~ 0.5 at.-%). Even very small fractions of Al in the films result in a significant change in film structure, with the films becoming amorphous with only 2 at.-% of Al in the film. After annealing in dry air (800 °C for 15 min), the films showed good dielectric properties, and after subtracting the series resistance of the silicon substrate and SiO_x interlayer capacitance, a dielectric constant for the Hf aluminate film of $\kappa \sim 10$ was calculated.[60]

Further information on the composition of the $(HfO_2)_x(Al_2O_3)_{1-x}$ films on Si(100) substrates was obtained using medium energy ion scattering (MEIS).[60] It was found that at low Al concentrations (10 at.-% and 21 at.-%), the $(HfO_2)_x(Al_2O_3)_{1-x}$ films crystallize on annealing at 1000 °C leading, in turn, to a marked increase in the thickness of a SiO_2 interfacial layer. However, in high Al content $(HfO_2)_x(Al_2O_3)_{1-x}$ films (Al = 38 at.-%) crystallization is suppressed, so that there is no appreciable increase in the thickness of the SiO_2 interfacial layer after annealing.

2.3. MOCVD of Lanthanide Oxides

Although ZrO_2, HfO_2, and their related silicates have been the most intensively investigated materials for gate dielectric applications,[2] there has also been much recent interest in the rare-earth oxides.[61] The rare-earth oxides M_2O_3 (M = La, Pr, Gd, and Nd) are good insulators due to their large bandgaps (3.9 eV for Pr_2O_3, 5.6 eV for Gd_2O_3), have high dielectric constants (Gd_2O_3, $\kappa = 16$; La_2O_3, $\kappa = 27$; Pr_2O_3, $\kappa = 26$–30), and have good thermodynamic stability on silicon, making them attractive materials for high-κ dielectric applications.[2] Another attractive feature of some rare-earth oxides, such as Pr_2O_3 and Gd_2O_3, is their relatively close lattice match to silicon (e.g., $a(Gd_2O_3) = 10.812$Å; $2a(Si) = 10.862$Å), which offers the possibility of epitaxial growth, thereby eliminating problems related to grain boundaries in polycrystalline films. It has also been shown that Gd_2O_3 can be grown epitaxially on GaAs(100), to give an insulating and passivating oxide layer,[62] which has potential applications in a wide range of group III-V photonic and electronic devices.

The large radii of Ln^{3+} ions (e.g., six-coordinate radii: $La^{3+} = 117.2$ pm, $Pr^{3+} = 113$ pm, $Gd^{3+} = 107.8$ pm) presents a real challenge for the synthesis of volatile precursors for MOCVD; coordinative saturation requires either high coordination numbers (up to 12), or very sterically demanding ligands. High coordination numbers are often achieved by the formation of oligomeric species with bridging ligands, resulting in extremely low volatility.

The oldest known class of volatile lanthanide complexes is the *tris*-β-diketonates that have been known since the early years of the 20th century. They are easily prepared and have excellent ambient stability. [Ln(thd)$_3$] complexes have been investigated for MOCVD of oxides of La,[63,64] Pr,[65] Gd,[66] and Nd.[67] However these precursors are thermally quite robust and require high growth temperatures that are generally incompatible with microelectronics applications, where high growth temperatures can lead to problems such as increased dopant diffusion, and the oxide films produced are often contaminated with trace carbon. Fluorinated β-diketonate complexes such as [Pr(hfa)$_3$(diglyme)] (hfa=1,1,1,5,5,5-hexafluoropentane-2,4-dionate)[65] show enhanced volatility compared with non-fluorinated precursors, but the oxide films produced from these precursors contain high levels of fluorine.

A new class of volatile fluorine-free lanthanide β-ketoiminate complexes has been developed for the MOCVD of lanthanide oxides. The complexes [Ln(^{t}BuMeMe)$_3$] (Ln = Ce, Nd, Gd, Er), [Ln(^{t}BuEtMe)$_3$] (Ln = Nd, Er), and [Er(^{t}Bu^{t}BuMe)$_3$] are coordinatively saturated monomers, and [Ce(^{t}BuMeMe)$_3$] was used to deposit CeO_2 thin films by pulsed MOCVD.[68]

The lanthanide *tris*-silylamides [Ln{N(SiMe$_3$)$_2$}$_3$] were the first example of monomeric three-coordinate lanthanide complexes,[69] and they show reasonable volatility. We found that MOCVD using these precursors resulted in variable incorporation of silicate into the oxide film.[70] Simple Si-free alkylamides of the lanthanides (e.g., [Ln(N^{i}Pr$_2$)$_3$(THF)]) are not sufficiently volatile to be used in MOCVD and so there are, as yet, no suitable amide precursors for MOCVD of lanthanide oxides.

The donor-functionalized [mmp] ligand might be expected to form monomeric $[Ln(mmp)_3]$ complexes with the lanthanides. However, it has been shown that the late lanthanides form dimeric complexes, and $[Lu(mmp)_3]_2$ has been characterized by XRD.[71] Despite their dimeric structure, these complexes show some volatility and are therefore candidates for MOCVD of lanthanide oxides. Our interest has been primarily in the early lanthanides, and we found that the mmp complexes of these metals were unstable in solution, condensing to form species with extremely complex ^1H NMR spectra and very low volatility. Elemental analysis indicated that these species are oxo-bridged clusters of general formula $[Ln(mmp)_2]_nO_{n/2}$. We have discovered that this condensation reaction is inhibited in the presence of 3 mol. equiv. tetraglyme/$Ln(mmp)_3$ or 1 mol. equiv. of [Hmmp].[72] ^1H NMR studies of a $[Pr(mmp)_3]$/tetraglyme/toluene solution indicated that tetraglyme is not coordinated directly to Pr, but is in the outer sphere of the complex. This suggests that the presence of the tetraglyme prevents the inner sphere interaction of $[Pr(mmp)_3]$ moieties necessary for the unwanted condensation reaction to occur. ^1H NMR spectroscopy has also shown that an anhydrous solution of $[La(mmp)_3]$/3 tetraglyme is indefinitely stable at room temperature, and we have used toluene solutions of $[Ln(mmp)_3]$/3 tetraglyme to grow oxide films of La,[73] Pr,[74,75] Nd,[76] and Gd,[77] containing very little or no detectable carbon, even in the absence of O_2. The decomposition of these $[Ln(mmp)_3]$ complexes may be analogous to that of $[Hf(mmp)_3]$ (Reaction 1), resulting in the formation of some $Ln(OH)_3$ in the films. This would be consistent with the frequent observation of excess O in our films. These results will be discussed in more detail below.

2.3.1. MOCVD of Praseodymium Oxide

Pr has a stable +4 oxidation state, and so a range of oxides (PrO_2, Pr_6O_{11}, and Pr_2O_3) as well as intermediate compositions are available. Pr_2O_3 is of the greatest interest due to the close lattice of the cubic C form to Si. We have used $[Pr(mmp)_3]$/3 tetraglyme to grow thin films of praseodymium oxides on Si(100) over a wide range of substrate temperatures from 250 to 600 °C.[74]

XRD data for PrO_x films deposited between 400 and 550 °C in the presence of oxygen indicated that the layers were comprised predominantly of the β-Pr_6O_{11} phase. Analysis of the Pr_6O_{11} films by scanning electron microscopy (SEM) showed that all the as-grown films exhibited a columnar growth habit.

2.3.2. MOCVD of Gadolinium Oxide

We have also used toluene solutions of $[Gd(mmp)_3]$/tetraglyme to grow thin films of gadolinium oxide on both Si(100) and GaAs(100) substrates over a wide range of temperatures from 300 °C to 600 °C.[77] Significantly, carbon was absent from all the films at the estimated AES detection limit of < 0.5 at.-%, even when the films were grown in the absence of O_2.

XRD data for Gd_2O_3 films showed that at growth temperatures above 450 °C, the GdO_x films were crystalline Gd_2O_3 with a C-type structure exhibiting a preferred (111) orientation. At lower growth temperatures the data showed no diffraction features, suggesting an amorphous disordered structure. The XRD data of a Gd_2O_3 film deposited on GaAs(100) at 450 °C was dominated by the (222) reflection, indicating a strong preferred orientation or even a heteroepitaxial relation with the underlying GaAs.[77] SEM images of fracture cross-sections from Gd oxide films deposited at 450/C on GaAs(001) and Si(001) substrates showed that, in both cases, the microstructure is featureless on the micrometer scale.

2.3.3. MOCVD of Lanthanum Oxide

As in the case of gadolinium oxide, lanthanum oxide films grown from $[La(mmp)_3]$/tetraglyme were carbon-free,[73] and the XRD data of a film deposited at 450 °C were consistent with the random powder diffraction pattern of La_2O_3 with a hexagonal structure. A SEM image of a fracture sample from a typical lanthanum oxide film deposited at 450 °C showed a columnar growth habit, similar to the morphology of Pr_6O_{11} films.

2.3.4. MOCVD of Neodymium Oxide

Carbon-free neodymium oxide films were grown on both Si(100) and GaAs(100) substrates using toluene solutions of $[Nd(mmp)_3]$/tetraglyme at temperatures ranging from 250 to 550 °C.[76] XRD data showed that, at growth temperatures above 450 °C, the Nd_2O_3 films on Si(100) were crystalline, with a C-type structure exhibiting a preferred (100) orientation. At lower growth temperatures, the data show no diffraction features, characteristic of an amorphous disordered structure. Nd_2O_3 films grown on GaAs(100) at 450 °C also demonstrated a C-type crystalline structure, but became amorphous at higher growth temperatures, possibly due to a surface reaction or degradation.

SEM images of Nd oxide films deposited at 450 °C on Si(100) and GaAs(100) showed that, in both cases, the microstructure is featureless, in contrast to the columnar La_2O_3 films deposited on Si(100) using $[La(mmp)_3]$/tetraglyme.

2.3.5. MOCVD of $LaAlO_3$

Lanthanum aluminum oxide is a potential substrate, or buffer layer for a variety of perovskite films (e.g., supercon-

ductors, ferroelectrics, metal conducting oxides),[78] and has also attracted much recent attention as an alternative high-κ gate dielectric material.[2] The β-diketonates [La(thd)$_3$] and [Al(thd)$_3$] have been used for the MOCVD of $LaAlO_3$,[79,80] whilst [La(thd)$_3$] (thd = 2,2,6,6-tetramethylheptane-3,5-dionate),[81] [La[N(SiMe$_3$)$_2$]$_3$],[82] and [La(^{i}PrAMD)$_3$] (^{i}PrAMD = *N,N'*-diisopropylacetamidinatonate) with [AlMe$_3$][83] have been utilized in ALD.

We have recently used the "single-source" alkoxide precursor [LaAl(O^{i}Pr)$_6$(^{i}PrOH)]$_2$ to deposit $LaAlO_3$ by liquid-injection MOCVD.[84] The complex is a centrosymmetric dimer with six-coordinate La and four-coordinate Al atoms (see Fig. 9). The two La atoms are linked by two bridging isopropoxide ligands, and each La atom is linked by a further two bridging isopropoxide ligands to an Al atom. The coordination geometry at La is highly distorted octahedral. The advantages of using alkoxide precursors rather than β-diketonates include lower deposition temperatures and reduced carbon contamination,[26] whilst the use of a single-source precursor containing the metals in the ratio required in a complex solid oxide offers the potential of improved stoichiometry control, especially in the growth of complex oxides by liquid-injection MOCVD where the use of a single evaporator generally necessitates careful matching of precursor evaporation and deposition characteristics.[26]

The $LaAlO_3$ films were deposited over a wide range of substrate temperatures (350–550 °C).[84] Energy dispersive X-ray (EDX) data showed that the films had variable La/Al ratios (0.48–1.03), with the optimum deposition temperature range for the required 1:1 ratio being 450–500 °C, with an argon flow rate of 400cm^3 min^{-1} and an oxygen flow rate of 100 cm^3 min^{-1}. At higher substrate temperatures (500–550 °C) the films became La deficient. This may be due to decomposition of the precursor, leading to partial separation of the La and Al components and pre-deposition of involatile La-oxide. XRD showed that films deposited at 500 and 550 °C were essentially amorphous.

3. ALD of Dielectric Oxides

3.1. Conventional ALD of ZrO_2 and HfO_2

Crystalline ZrO_2 and HfO_2 films have been grown by ALD using the halides $ZrCl_4$,[85] ZrI_4,[86] $HfCl_4$, and HfI_4.[87–90] In contrast to MOCVD, the high thermal stability of metal halides is an advantage in ALD, as exchange reactions between reactive MX_n moieties and surface [OH] species predominate over thermal-decomposition reactions, and so halide precursors show good self-limiting growth behavior. Although Zr and Hf halides have given pure oxide films by ALD, they are high-melting-point solid sources, and so there is the risk of particle transport to the substrate. The chemical purity of metal halides can be questionable as they are difficult to purify, and halide contamination is potentially a serious problem in microelectronics applications.

Although the use of [Cp$_2$ZrMe$_2$] in MOCVD leads to heavily carbon-contaminated ZrO_2 films,[91] both [Cp$_2$ZrMe$_2$][92] and [Cp$_2$HfMe$_2$][93] give good self-limiting ALD growth at an optimum growth temperature of 350 °C. In this case, the ZrO_2 and HfO_2 films were high purity with non-detectable carbon and hydrogen.

Recently it has been shown that metal alkylamides [M(NR$_2$)$_4$] give self-limiting ALD growth,[94] and high-purity HfO_2 has been deposited by ALD using [Hf(NEtMe)$_4$].[95] However, the relatively low strength of the [Hf-N] bond restricts the ALD growth temperature to 250–300 °C, which can lead to the incorporation of mobile ion impurities, such as [OH] or [H], in the oxide film.[27]

The use of high-purity metal alkoxides potentially offers process advantages over halide precursors, and the higher strength of the [M-O] bond relative to [M-N] may allow the use of higher growth temperatures, with a corresponding reduction in impurity incorporation. Zirconium tetra-*tert*-butoxide, [Zr(O^{t}Bu)$_4$] has recently been used for the ALD of ZrO_2 using H_2O as the oxygen source.[96] The films

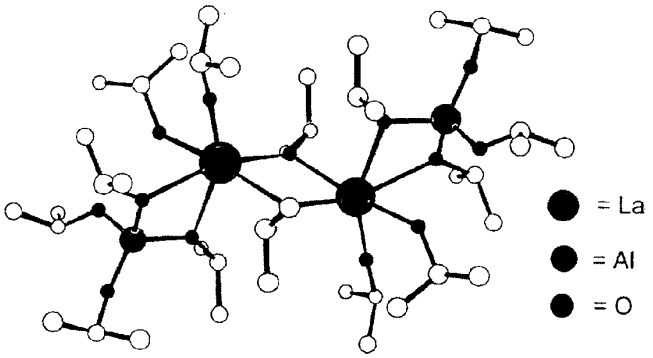

Fig. 9. Crystal structure of [LaAl(O^{i}Pr)$_6$(^{i}PrOH)]$_2$. Reproduced with permission from [84]; copyright 2005, Royal Society of Chemistry.

obtained were high quality, with permittivities as high as 32, comparing favorably with the permittivities of 18–24 obtained using halide precursors. However $[Zr(O^tBu)_4]$ failed to give truly self-limiting growth due to decomposition of the precursor.

A number of new zirconium and hafnium alkoxide ALD precursors containing alternative alkoxide groups to $[O^tBu]$ have therefore been examined in an effort to stabilize the precursor to surface decomposition, and to modify its reactivity towards surface [OH] species. The deposition of ZrO_2 has been achieved using $[Zr(O^tBu)_2(dmae)_2]$,[53,97] $[Zr(O^iPr)_2(dmae)_2]$,[97] and $[Zr(dmae)_4]$[97] (dmae = $OCH_2CH_2NMe_2$), but none of the complexes displayed self-limiting growth and in each case the oxide growth rate increased with increasing precursor pulse length. This can be attributed to the decomposition of the alkoxide groups on growth surface. The decomposition reaction could, however, be controlled by using low growth temperatures (240 °C) and short precursor pulses (0.2 s).

HfO_2 films have been deposited by ALD from $[Hf(mmp)_4]$ and H_2O in the temperature range 275–425 °C on borosilicate glass and Si(100) substrates,[98] although film growth was not entirely self-limiting with the oxide growth rate increasing with increasing precursor pulse length (see Fig. 10b), due to the decomposition of the precursor. Similarly, the heteroleptic Hf alkoxide precursor $[Hf(O^tBu)_2(mmp)_2]$ also failed to give fully self-limiting growth of HfO_2 by ALD (see Fig. 10a).[99] The refractive index was found to be a function of film density, and both $[Hf(mmp)_4]$ and $[Hf(O^tBu)_2(mmp)_2]$ gave less dense films (refractive indices < 2) than those grown from $HfCl_4$ (refractive indices ~ 2.0–2.2).[88] The decomposition of both $[Hf(mmp)_4]$ and $[Hf(O^tBu)_2(mmp)_2]$ could be significantly reduced by lowering the substrate temperature to < 300 °C, giving growth rates that were less dependent on precursor pulse length. However, at these low growth temperatures, the growth rate from these precursors became very low (~ 0.02–0.03 nm per cycle from $[Hf(mmp)_4]$ and ~ 0.04–0.06 nm per cycle from $[Hf(O^tBu)_2(mmp)_2]$), probably due to steric inhibition of the surface exchange reaction between [OH] species and $[Hf(mmp)_x]$ precursor moieties (see below).

C-V data for a $[Al/HfO_2/SiO_2/p\text{-}Si(100)]$ MOS structure deposited from $[Hf(mmp)_4]$ at 360 °C showed that the HfO_2 films had good dielectric properties with clear accumulation, inversion, and depletion regions at negative biases. The *C-V* curves of the as-deposited films showed clockwise hysteresis, attributable to the presence of mobile positive charge in the films.[98] The flat-band voltage of the *C-V* curves of as-deposited films was shifted to positive bias from the expected value of –0.9 V to –0.1 V by approx. 0.5 V, indicative of electron traps. The *C-V* behavior of the HfO_2 films improved after annealing, with a marked decrease in hysteresis.

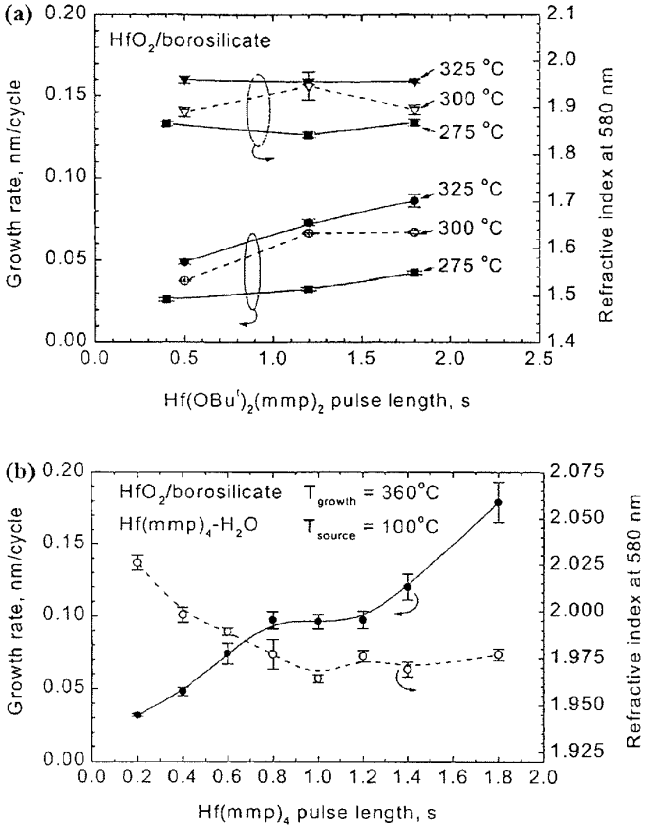

Fig. 10. Variation in film growth rate and refractive index with precursor pulse length for HfO_2 films grown by conventional ALD at various substrate temperatures using (a) $[Hf(O^tBu)_2(mmp)_2]$ (reprinted from [99]) and (b) $[Hf(mmp)_4]$ (reproduced with permission from [98]; copyright 2003, Royal Society of Chemistry).

3.2. Liquid-Injection ALD of HfO_2

In conventional ALD, the metal-organic precursor is evaporated from an open boat or "bubbler" held at high

temperature (typically 170–200 °C) for the duration of the ALD growth studies. This must inevitably lead to varying degrees of thermal decomposition of less thermally stable precursors such as metal alkylamides and alkoxides. The use of liquid-injection techniques, in which the precursor is held in solution at room temperature until evaporation, avoids this problem and therefore allows the use of less volatile precursors. Surprisingly there have been very few reports to date using "liquid-injection ALD" for the growth of dielectric oxides. Potentially, liquid-injection ALD has a number of advantages over conventional ALD using continuously heated open boats or "bubblers". These are:

- The precursor solution is held at room temperature prior to evaporation, which avoids thermal decomposition of the precursor.
- "Point of use" evaporation allows the use of higher evaporator temperatures and thus a wider choice of precursor is available.
- It is possible to carry out ALD and MOCVD on the same reactor, providing information about the "thermal" window for ALD growth.
- It should be possible to carry out ALD using a "cocktail" of precursors in solution, making it easier to grow complex oxides and doped materials such as Hf silicates and aluminates.

The effect of growth temperature on the ALD deposition rate of HfO_2 using a solution of $[Hf(mmp)_4]$ in pentane is shown in Figure 11, along with the equivalent MOCVD data.[100] The growth rates have been normalized with respect to moles of injected precursor to allow a direct comparison. At low growth temperatures (up to ~275 °C) little change is observed in the growth rate. However, between 275 and ~350 °C a clear increase is seen, indicative of thermal decomposition of the precursor. Omitting the water-vapor pulses from the ALD cycle at 325 °C effectively suppresses the deposition.

The variation of growth rate with precursor volume injected per ALD cycle is shown in Figure 12 for $[Hf(mmp)_4]$. In fully self-limiting ALD the growth per cycle would be expected to increase with injected precursor volume until surface saturation is achieved,[27] after which the growth rate should become constant. At 225 °C there appears to be a weak onset of self-limiting growth for the $[Hf(mmp)_4]$ at precursor volumes of between 20–25 μL per cycle. However, the growth rate clearly continues to increase with injected volume, indicating that self-limiting growth is not actually achieved.

These results parallel those obtained using $[Hf(mmp)_4]$ in conventional ALD, albeit at higher substrate temperatures (360 °C),[98] in which a self-limiting growth plateau was observed at intermediate precursor pulse lengths (0.8–1.2 s), but at long precursor pulse lengths (> 1.4 s) there was a rapid increase in oxide growth rate. A breakdown of self-limiting growth at substrate temperatures below the precursor's thermal decomposition point (e.g., 250–300 °C) has also been observed in conventional ALD for a wide range of Zr and Hf alkoxides. These include $[Zr(O^tBu)_2(dmae)_2]$,[97] $[Zr(O^iPr)_2(dmae)_2]$,[97] $[Zr(dmae)_4]$,[97] $[Hf(O^tBu)_2(mmp)_2]$,[99] and $[Hf(mmp)_4]$,[98] and can be attributed to decomposition of the precursor to create reactive [M-OH] surface sites. This will be discussed more fully in the general discussion of ALD mechanisms in Section 3.3.3.

The composition of the HfO_2 films grown by ALD and MOCVD was determined by AES, which showed that the purity of the ALD films, with residual carbon levels in the range 0.8–2.5 at.-%, is equal to or better than the films deposited by MOCVD. The purity also compares favorably

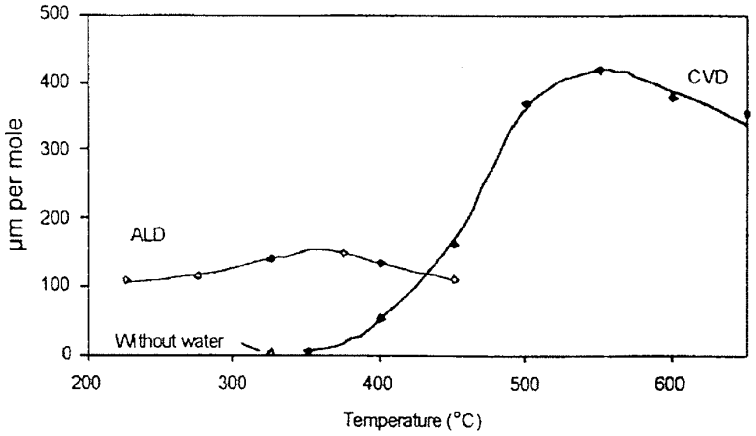

Fig. 11. Variation in growth rate with substrate temperature for HfO_2 grown by liquid-injection ALD and MOCVD using a solution of $[Hf(mmp)_4]$ in pentane (reprinted from [100]).

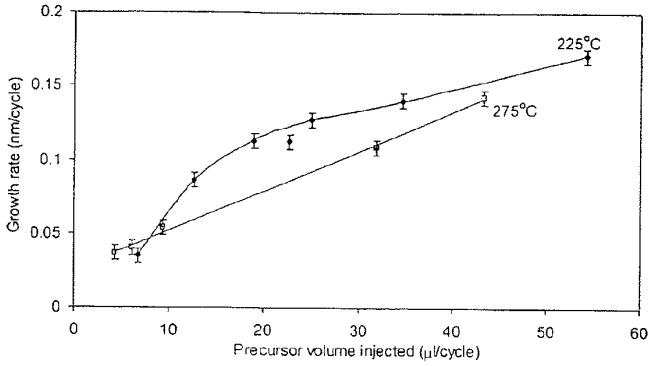

Fig. 12. Variation in growth rate with precursor volume injected per growth cycle for HfO_2 grown by liquid-injection ALD using a solution of $[Hf(mmp)_4]$ in heptane (reprinted from [100]).

with films grown by conventional ALD using $[Hf(mmp)_4]$ (C = 2.2–6 at.-%, determined by time of flight-elastic recoil detection analysis (TOF-ERDA)),[98] showing that the heptane solvent does not contribute any significant level of carbon to the films.

3.3. Liquid-Injection ALD of Lanthanide Oxides

There are few precursors available for the ALD of rare-earth oxides. The simple lanthanide alkylamides $[Ln(NR_2)_3]$ are unstable and involatile. Metal β-diketonates have been investigated,[101,102] but ozone is required to get acceptable growth rates. Recently, metal amidinates, $[M(R\text{-}R'AMD)_n]$ (M=Ti, V, Mn, Fe, Co, Ni, Cu, Ag, La; R=^{i}Pr, ^{t}Bu; R'=Me, ^{t}Bu) have been proposed as a general class of precursors for the ALD of metal and metal oxide films,[103] and La_2O_3 has been deposited by ALD using $[La(^iPr)NC(CH_3)N(^iPr)]$.[104] A recent patent describes the use of *tris*-cyclopentadienyl lanthanide complexes for the deposition of a large range of lanthanide oxides by ALD.[105]

The lanthanide alkyl silylamides, $[Ln[N(SiMe_3)_2]_3]$, are also volatile and relatively stable,[69] but recent ALD studies[106] showed that $Pr[N(SiMe_3)_2]_3$ produced a Pr silicate, $PrSi_xO_y$, rather than a pure oxide film, and so we have concentrated our investigations on the Si-free alkoxides $[Ln(mmp)_3]$ (Ln = Gd, Pr).

3.3.1. Liquid-Injection ALD of Gd_2O_3 Films

Gd_2O_3 thin films were deposited by liquid-injection ALD between 200 °C and 300 °C using a 0.05M solution of $[Gd(mmp)_3]$ in toluene with 3 mol. equiv. of tetraglyme added to stabilize the precursor solution.[100] The variation in growth rate with substrate temperature is shown in Figure 13, and for comparison the MOCVD data are also presented. The ALD oxide growth rate remains effectively constant with increasing temperature in the substrate temperatures range 200–250 °C. However, above 250 °C the growth rate starts to increase; this can be attributed to thermal decomposition of the $[Gd(mmp)_3]$. The variation of the Gd_2O_3 growth rate with precursor volume injected per ALD cycle (Fig. 14), shows that even at a substrate temperature as low as 225 °C, oxide growth is not self-limiting due to precursor decomposition.

The composition of the Gd_2O_3 films grown by ALD and MOCVD was determined by AES, and this showed that the ALD and MOCVD films were of comparable purity, with carbon not detected in any of the films.[100] As Gd_2O_3 is the only stable stoichiometry of gadolinium oxide, the O/Gd ratios of 1.7–2.0 indicate that the films contain excess oxygen (expected O:Gd ratio in Gd_2O_3 = 1.5). Significantly, carbon was absent from all of the films at the estimated AES detection limit of < 0.5 at.-%.

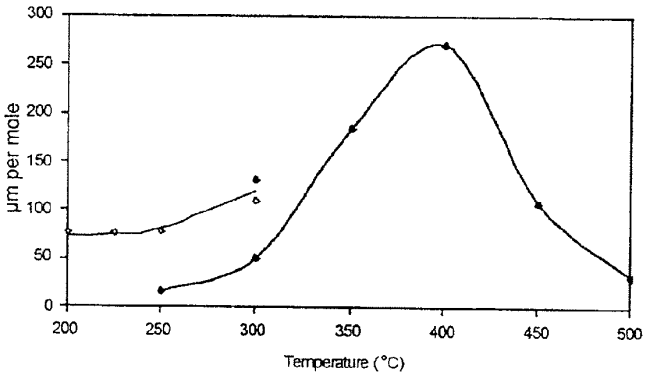

Fig. 13. Variation in growth rate with substrate temperature for Gd_2O_3 grown by liquid-injection ALD and MOCVD using a $[Gd(mmp)_3]$/3 tetraglyme/toluene solution (reprinted from [100]).

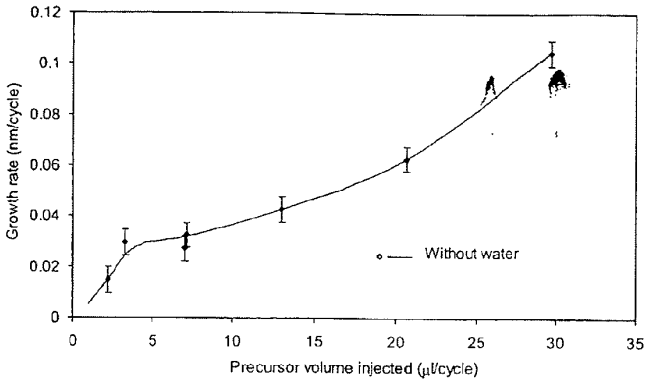

Fig. 14. Variation in growth rate with precursor volume injected per growth cycle for Gd_2O_3 grown by liquid-injection ALD using a [Gd(mmp)$_3$]/3 tetraglyme/toluene solution (reprinted from [100]).

XRD analysis of the as-grown Gd_2O_3 films deposited by ALD at 225 °C showed some crystallinity (see Fig. 15), giving the characteristic (222), (440), and (622) reflections of C-type Gd_2O_3. The same phase was observed in Gd_2O_3 deposited at >450 °C by liquid-injection MOCVD using

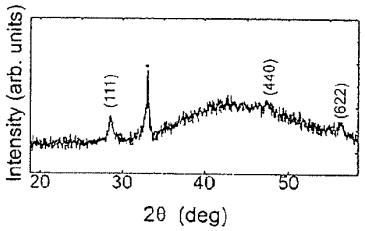

Fig. 15. XRD data for a Gd_2O_3 film (~50 nm) deposited by ALD at 225 °C using 900 ALD cycles. * Si(200) peak (reprinted from [100]).

[Gd(mmp)$_3$].[77] The width of the diffraction peaks is indicative of nanoscale crystalline domains. SEM images of the Gd_2O_3 films deposited at 225 °C showed a generally featureless morphology, consistent with the XRD data.

3.3.2. Liquid-Injection ALD of PrO_x

PrO_x films were deposited by ALD between 200 and 300 °C using a solution of [Pr(mmp)$_3$] in toluene with 3 mol. equiv. of added tetraglyme.[100] The variation in ALD and MOCVD growth rates with substrate temperature is shown in Figure 16. In this case, the PrO_x growth rate tends to increase with substrate temperate over the full temperature range 150–350 °C. However, the increase is most rapid in the region 250–350 °C, mirroring the MOCVD growth data. The variation in growth rate with precursor volume injected per ALD cycle is shown in Figure 17. The data indicate that growth is not self-limiting due to precursor decomposition, and that the growth rate is negligible in the absence of added water.

XRD data for a PrO_x films deposited at 225 °C (Fig. 18) showed that they had some crystalline structure. It was not possible to make an unambiguous assignment; however, the diffraction peaks are consistent with the (222) and (400) reflections of Pr_2O_3. It is significant that growth of PrO_x by liquid-injection MOCVD at 450–550 °C gave predominantly the oxygen-rich Pr_6O_{11} phase.[74] The reason for this difference may be due to removal of the oxygen-rich [mmp] ligand in ALD by reaction with surface [OH] to produce species such as [Pr(OH)$_{3-n}$], i.e., an environment with less available oxygen. SEM data for the PrO_x films showed that they have a very smooth surface morphology with no obvious crystalline structure.

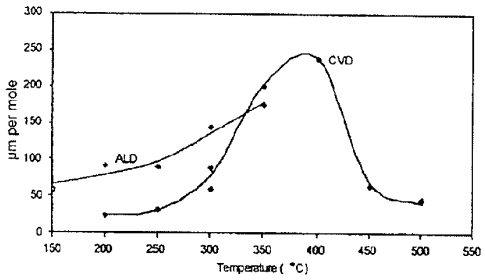

Fig. 16. Variation in growth rate with substrate temperature for PrO_x grown by liquid-injection ALD and MOCVD using a [Pr(mmp)$_3$]/3 tetraglyme/toluene solution (reprinted from [100]).

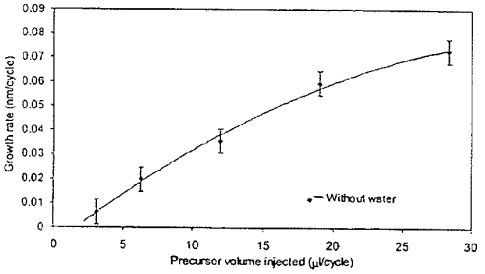

Fig. 17. Variation in growth rate with precursor volume injected per growth cycle for PrO_x grown by liquid-injection ALD using a [Pr(mmp)$_3$]/3 tetraglyme/toluene solution (reprinted from [100]).

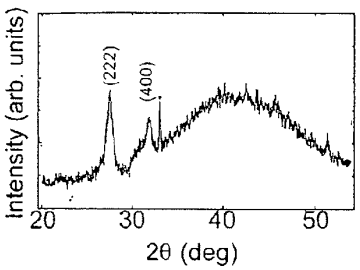

Fig. 18. XRD data for PrO_x films grown by liquid-injection ALD using a $[Pr(mmp)_3]$/3 tetraglyme/toluene solution (reprinted from [100]).

AES data for the PrO_x deposited by ALD and MOCVD from $[Pr(mmp)_3]$ indicated that the purity of the ALD films was equal to the MOCVD films, with carbon levels varying from non-detected to 3.3 at.-%. The O/Pr ratio varies from 1.7–2.5, but the AES data did not allow the unambiguous assignment of the films as the Pr_2O_3 (O/Pr = 1.5) or Pr_6O_{11} (O/Pr = 1.8) phase.

3.3.3. Growth Mechanisms in the ALD of Dielectric Oxides

It is clear from our studies and those of other workers that self-limiting ALD growth is seldom achieved using metal alkoxide precursors, whereas good self-limiting growth can be achieved using metal halides and metal alkylamides. We propose that four major factors control the decomposition of alkoxide precursors in ALD:

1. Ease of β-hydride elimination of alkoxide groups on the growth surface. This will be a major factor controlling precursor decomposition at low substrate temperatures (e.g., 225–300 °C)
2. Steric shielding by residual surface-bound alkoxide ligands of reactive [O-M-OH] surface sites. This will inhibit the reactivity of the [M-OH] sites towards incoming $[M(OR)_x]$ precursor molecules.
3. Steric shielding by the (OR) ligands of the metal center in the $M(OR)_x$ precursor. This will significantly influence the surface exchange reaction between the $M(OR)_x$ molecule and surface-bound [OH] species.
4. Thermal stability of [M-OR] bonds on the growth surface will be a significant factor controlling precursor decomposition at higher substrate temperatures (e.g., > 350 °C).

These factors are discussed in detail below.

β-Hydride Elimination of Alkoxide Ligands: The first alkoxide studied in ALD was $[Zr(O^tBu)_4]$, in combination with H_2O.[96] Although ZrO_2 films of good dielectric quality ($\kappa \sim 30$) and reasonable purity (C ~ 2–6 at.-%) were deposited, growth was not self-limiting, with the growth per cycle showing a marked increase with increasing precursor pulse length.[96] It has been established that H_2O plays a key role in the growth process,[107] as shown in Reactions 2, 3, when (s) indicates a surface-bound species.

$$-(OH)(s) + Zr(O^tBu)_4 \rightarrow -O-Zr(O^tBu)_3(s) + {}^tBuOH \rightarrow (CH_3)_2C{=}CH_2\uparrow + H_2O\uparrow \quad (2)$$

$$-O-Zr(O^tBu)(s) \rightarrow -O-Zr-(OH)(s) + (CH_3)_2C{=}CH_2\uparrow \quad (3)$$

The initial step in the H_2O – assisted heterogeneous decomposition of $[Zr(O^tBu)_4]$ is the reaction between surface bound [OH] groups and $[Zr(O^tBu)_4]$ molecules to liberate tert-butanol. This can then decompose to iso-butylene and generate H_2O to give a self-propagating chain reaction. This in itself would lead to a breakdown of self-limiting growth, however another crucial factor in the breakdown of self-limiting growth is step 2, in which the remaining $[O^tBu]$ groups undergo an internal β-hydride elimination to liberate isobutylene and form **Zr-OH** species. These will be highly reactive sites towards incoming $[Zr(O^tBu)_4]$ molecules and will be continuously generated throughout the ALD growth process, making self-limiting growth impossible.

Recent ALD studies [108] using in situ quadrupole mass spectroscopy (QMS) and a quartz crystal microbalance (QCM) showed that $[Zr(O^tBu)_2(dmae)_2]$, $[Zr(O^iPr)_2(dmae)_2]$, and $[Zr(dmae)_4]$ (dmae = $OCH_2CH_2NMe_2$) all fail to give self-limiting growth. Significantly, it was found that growth did not occur without an initial water pulse, but after this initial surface hydroxylation step QCM studies showed that there was a continual oxide mass gain in the absence of any further water pulses. This can be explained by the mechanism for the decomposition of $[Zr(O^iPr)_2(dmae)_2]$ (Reactions 4, 5).

$$-(OH)(s) + Zr(O^iPr)_2(dmae)_2 \rightarrow -O-Zr(O^iPr)_2(dmae)(s) + Me_2NCH_2CH_2OH\uparrow \quad (4)$$

$$\text{or } \rightarrow -O-Zr(O^iPr)(dmae)_2(s) + (CH_3)_2COH\uparrow$$

$$-O-Zr(O^iPr)(s) \rightarrow -O-Zr-OH(s) + CH_2{=}CH(CH_3)\uparrow \quad (5)$$

$$-O-Zr(OCH_2CH_2NMe_2)(s) \rightarrow -O-Zr-OH(s) + CH_2{=}CHNMe_2\uparrow$$

The reaction between the incoming $[Zr(O^iPr)_2(dmae)_2]$ precursor molecule and surface-bound [OH] species leads to elimination of either ^iPrOH or dmaeH and chemisorption of the precursor (step 1). Subsequent decomposition of the [Zr-**O^{i}Pr**] or [Zr-**dmae**] groups on the surface by β-hydride elimination liberates an alkene and generates reactive Zr-OH surface sites in the absence of added H_2O.

The failure of $[Hf(mmp)_4]$ to achieve self-limiting growth (see Fig. 10b) can be attributed to the β-hydride elimination of [mmp] to generate [Hf-OH] surface species (see Reaction 1). The related precursor $[Hf(O^tBu)_2(mmp)_2]$ also fails to give self-limiting growth at 275–325 °C in conventional ALD,[99] and this can again be attributed to the β-hydride elimination of $[O^tBu]$ and [mmp] groups (see Schemes 1 and 3) to generate [Hf-OH] reactive sites.

By analogy, $[Gd(mmp)_3]$ and $[Pr(mmp)_3]$ can be expected to generate Ln_2O_3 and $Ln(OH)_x$ species, prohibiting self-limiting growth, and this allows us to rationalize the data shown in Figures 14 and 17. Further support for the role of β-hydride elimination in alkoxide decomposition is the recent observation that $[Ti(OMe)_4]$, which has no β-hydrogen atoms, gives good self-limiting ALD growth at 250 °C.[109]

The negative effect of the β-hydride elimination reaction on the ALD process can be contrasted with its positive effect on MOCVD, where it promotes the formation of carbon-free films.

Steric Factors: As well as the tendency of the $[M(OR)_x]$ species to undergo β-hydride elimination on the growth surface, steric effects on the growth surface are likely to play a key role in ALD growth using alkoxide precursors. It has been shown that, even though both molecules contain a β-hydrogen, $[Ti(O^iPr)_4]$ [109] and $[Ti(OEt)_4]$[109] give reasonable self-limiting ALD growth at 300 °C, in contrast to Zr and Hf alkoxides, such as $[Zr(O^tPr)_2(dmae)_2]$ and $[Hf(mmp)_4]$. $[Ta(OEt)_5]$ also gives self-limiting growth at substrate temperatures below 350 °C.[110] This suggests that steric shielding of reactive [M-OH] surface sites by residual surface-bound [OR] ligands may be a key factor in allowing self-limiting growth. This will depend on the atomic radius of the metal center, number of residual alkoxide ligands, and the bulk of residual alkoxide ligands.

This proposal is supported by the approach to self-limiting growth by $[Hf(mmp)_4]$ (see Figs. 10b and 12). The conventional ALD data was obtained at the relatively high substrate temperature of 360 °C,[98] where thermal decomposition of the precursor is likely to be a contributing factor to the breakdown of self-limiting growth. It was anticipated that self-limiting growth would be obtained from $[Hf(mmp)_4]$ in the normal ALD "temperature window" of 250–300 °C, but only very low growth rates (~0.02nm per cycle) were obtained at substrate temperatures of 300 °C. This can be attributed to steric shielding of the Hf center in the $[Hf(mmp)_4]$ molecule by the bulky mmp ligands, which inhibits the exchange reaction between $Hf(mmp)_4$ and [OH] groups on the growth surface and drastically reduces the ALD growth rate.

The significant influence of steric effects on the ALD process is illustrated by the trend in growth rates at 300 °C which increases in the order $[Hf(mmp)_4]$ (~0.02 nm per cycle),[98] < $[Hf(O^tBu)_2(mmp)_2]$ (0.04–0.06 nm per cycle),[99] < $[Hf(ONEt_2)_4]$ (0.05–0.06 nm per cycle)[111] < $[Hf(NR_2)_4]$ (0.09 nm per cycle).[95] At a given temperature, the Hf-mmp complexes give the lowest growth rates, as steric shielding of the Hf center by the bulky bidentate mmp ligands lowers the reactivity of the precursor to surface [OH] species. The $[Hf(ONEt_2)_4]$ ligand has the potential to be bidentate and is likely to shield the Hf center more effectively than monodentate $[NR_2]$ ligands. The reactivity of $[Hf(ONEt_2)_4]$ towards surface [OH] (and the subsequent HfO_2 growth rate) is, therefore, lower than from $[Hf(NR_2)_4]$ precursors.

Once again, it is interesting to note the different requirements of ALD and MOCVD precursors, in that the steric shielding of the metal centers which lowers ALD growth rates to prohibitively low levels is a benefit in an MOCVD precursor (in which reduced reactivity towards [OH] or H_2O is an advantage).

Thermal Decomposition: In the case of the precursors investigated here, homolytic fission of the [M-OR] bond at the growth surface will inevitably become a significant factor at substrate temperatures over 350 °C, above the onset temperature of oxide growth by "thermal" MOCVD (see Figs. 13 and 16). At intermediate temperatures (~300 °C) precursor decomposition is likely to be governed by a combination of homolytic fission of the [M-OR] bond and β-hydride elimination of the alkoxide ligand, while at still lower temperatures (225–275 °C), β-hydride elimination will become the most significant factor leading to precursor decomposition and the breakdown of self-limiting growth. This is supported by the fact that $[Zr(NR_2)_4]$ and $[Hf(NR_2)_4]$ lead to good self-limiting ALD growth in the range 250–300 °C, despite the lower strength of the [Zr-N] and [Hf-N] bonds relative to [Zr-O] and [Hf-O] bonds.

4. Conclusions

The use of new metal alkoxide precursors specifically designed for MOCVD has resulted in significant process improvements and better-quality dielectric oxides. MOCVD precursor properties and decomposition characteristics have been modified and improved by the addition of bidentate donor-functionalized alkoxide groups such as [mmp] and [dmop]. However, due to the very different requirements of MOCVD and ALD precursors, the use of these sterically demanding ligands has not been as successful in ALD as the decreased reactivity of the precursor towards oxygen nucleophiles leads to a severe inhibition of growth rates, and the tendency of these ligands to undergo β-hydride elimination leads to the formation of reactive $M(OH)_x$ surface sites and a breakdown of self-limiting growth.

Received: February 28, 2005
Final version: July 18, 2005

[1] A. Packan, *Science* **1999**, *285*, 2079.
[2] G. D. Wilk, R. M. Wallace, J. M. Anthony, *J. Appl. Phys.* **2001**, *89*, 5243.
[3] T. M. Klein, D. Niu, W. S. Epling, W. Li, D. M. Maher, C. C. Hobbs, R. I. Hedge, I. J. R. Baumvol, G. N. Parsons, *Appl. Phys. Lett.* **1999**, *75*, 4001.
[4] M. Copel, M. A. Gribelyuk, E. Gusev, *Appl. Phys. Lett.* **2000**, *76*, 436.
[5] B. H. Lee, L. Kang, R. Nieh, W.-J. Qi, J. C. Lee, *Appl. Phys. Lett.* **2000**, *76*, 1926.
[6] G. D. Wilk, R. M. Wallace, *Appl. Phys. Lett.* **1999**, *74*, 2854.
[7] G. D. Wilk, R. M. Wallace, *Appl. Phys. Lett.* **2000**, *76*, 112.

[8] G. D. Wilk, M. L. Green, M.-Y. Ho, B. W. Busch, T. W. Sorsch, F. P. Klemens, B. Brijs, R. B. van Dover, A. Kornblit, T. Gustaffson, E. Garfunkel, S. Hellenius, D. Monroe, P. Kalavade, J. M. Hergenrother, *Tech. Dig. VLSI Symp.* **2002**, 88.
[9] M.-H. Cho, Y. S. Roh, C. N. Whang, K. Jeong, H. J. Choi, S. W. Nan, D.-H. Ko, *Appl. Phys. Lett.* **2002**, *81*, 1071.
[10] M. Wu, Y. Yang, A. Chin, W. J. Chen, C. M. Kwei, *IEEE Electron. Device Lett.* **2000**, *21*, 341.
[11] H. J. Osten, J. P. Liu, H. J. Mussig, *Appl. Phys. Lett.* **2000**, *80*, 297.
[12] J. Kwo, M. Hong, A. R. Kortan, K. T. Queeney, Y. J. Cabal, J. P. Mannaerts, T. Boone, J. J. Krajewski, A. M. Sergent, J. M. Rosamilia, *Appl. Phys. Lett.* **2000**, *77*, 130.
[13] J. A. Gupta, D. Landheer, J. P. McCaffrey, G. F. I. Sproule, *Appl. Phys. Lett.* **2001**, *78*, 1718.
[14] M. D. Kannan, S. K. Narayandass, C. Balasubramanian, D. Mangalaraj, *Phys. Stat. Solidi A* **1991**, *128*, 427.
[15] J.-H. Lee, J. P. Kim, J.-H. Lee, Y.-S. Kim, H.-S. Jung, N.-I. Lee, H.-K. Kang, K.-P. Suh, M.-M. Jeong, K.-T. Hyun, H.-S. Baik, Y. S. Chung, X. Liu, S. Ramanathan, T. Seidel, J. Winkler, A. Londergan, H. Y. Kim, J. M. Ha, N. K. Lee, *Proc. 2002 IEEE Int. Electron. Devices Meet.*, IEEE, Piscataway, NJ **2002**, pp. 221–224.
[16] S. Krupanidhi, N. Maffeo, M. Sayer, K. El-Assel, *J. Appl. Phys.* **1983**, *54*, 6601.
[17] K. Sreevinas, M. Sayer, D. J. Baar, M. Nishioka, *Appl. Phys. Lett.* **1988**, *52*, 709.
[18] K. Saenger, R. Roy, K. Etzold, J. Cuomo, *Mater. Res. Soc. Symp. Proc.* **1991**, *200*, 115.
[19] R. Ramesh, A. Inam, W. K. Chan, F. Tillerot, B. Wilkens, C. C. Chang, T. Sands, J. M. Tarascon, V. G. Keramidas, *Appl. Phys. Lett.* **1991**, *59*, 3542.
[20] K. D. Budd, S. K. Dey, D. A. Payne, *Br. Ceram. Soc. Proc.* **1985**, *36*, 107.
[21] R. W. Vest and J. Xu, *Ferroelectrics* **1989**, *93*, 21.
[22] M. de Keijser, G. J. M. Dormans, J. F. M. Gillessen, D. M. de Leeuw, H. W. Zandbergen, *Appl. Phys. Lett.* **1991**, *58*, 2636.
[23] M. de Keijser, G. J. M. Dormans, *Mater. Res. Soc. Bull.* **1996**, *21*, 37.
[24] A. C. Jones, *Chem. Vap. Deposition* **1998**, *4*, 169.
[25] I. M. Watson, *Chem. Vap. Deposition* **1997**, *3*, 9.
[26] A. C. Jones, *J. Mater. Chem.* **2002**, 12, 2576.
[27] M. Leskelä, M. Ritala, in *Handbook of Thin Film Materials*, Vol.1 (Ed: H. S. Nalwa), Academic Press, San Diego, CA **2002**, p. 103.
[28] R. N. Tauber, A. C. Dumbri , R. E. Caffrey, *J. Electrochem. Soc.* **1971**, *118*, 747.
[29] C. F. Powell, in *Chemically Deposited Nonmetals* (Eds: C. F. Powell, J. H. Oxley, J. M. Blocher), John Wiley & Sons Inc., New York **1966**, pp. 343-420.
[30] R. C. Smith, T. Ma, N. Hoilien, L. Y. Tsung, M. J. Bevan, L. Colombo, J. Roberts, S. A. Campbell, W. Gladfelter, *Adv. Mater. Opt. Electron.* **2000**, *10*, 105.
[31] M. Pulver, G. Wahl, in *Chemical Vapor Deposition–Proc. 14th Int. CVD Conf. and EUROCVD-11* (Eds: M. Allendorf, C. Bernard), The Electrochemical Soc., Pennington, NJ **1997**, Vol. 97-25, p. 960.
[32] A. C. Jones, T. J. Leedham, P. J. Wright, M. J. Crosbie, D. J. Williams, P. A. Lane, P. O'Brien, *Mater. Res. Soc. Proc.* **1998**, *495*, 11.
[33] M. Balog, M. Schieber, *J. Cryst. Growth* **1972**, *17*, 298.
[34] S. V. Pasko, L. G. Hubert-Pfalzgraf, A. Abrutius, P. Richard, A. Bartasyte, V. Kazlauskiene, *J. Mater. Chem.* **2004**, *14*, 1245.
[35] D. G. Colombo, D. C. Gilmer, V. G. Young Jr., S. A. Campbell, W. L. Gladfelter, *Chem. Vap. Deposition* **1998**, *4*, 220.
[36] A. Bastianini, G. A. Battiston, R. Gerbasi, M. Porchia, S. Daolio, *J. Phys. IV* **1995**, *5*, C5-525.
[37] Y. Oshita, A. Ogura, A. Hoshino, S. Hiiro, H. Machida, *J. Cryst. Growth* **2001**, *233*, 292.
[38] Y. Ohshita, A. Ogura, A. Hoshino, S. Hiiro, T. Suzuki, H. Machida, *Thin Solid Films* **2002**, *406*, 215.
[39] J. J. Gallegos, T. L. Ward, T. J. Boyle, M. A. Rodriguez, L. P. Francisco, *Chem. Vap. Deposition* **2000**, *6*, 21.
[40] D. C. Bradley, R. C. Mehrotra, D. P. Gaur, *Metal Alkoxides*, Academic Press, New York **1978**.
[41] H. J. Frenck, E. Oesterschulze, R. Beckmann, W. Kulisch, R. Kassing, *Mater. Sci. Eng.* **1991**, *A139*, 394.
[42] J. Gould, I. M. Povey, M. E. Pemble, W. R. Flavell, *J. Mater. Chem.* **1994**, *4*, 1815.
[43] Y. Takahashi, T. Kawae, M. Nasu, *J. Cryst. Growth* **1986**, *74*, 409.
[44] S. Pakswer, P. Skoug, in *Thin Dielectric Oxide Films Made By Oxygen Assisted Pyrolysis of Alkoxides* (Eds: J. M. Blocher, J. C. Withers), The Electrochemical Society, Los Angeles **1970**, p.619.
[45] D. C. Bradley, *Chem. Rev.* **1989**, *89*, 1317.
[46] A. C. Jones, T. J. Leedham, P. J. Wright, M. J. Crosbie, D. J. Williams, K. A. Fleeting, H. O. Davies, D. J. Otway, P. O'Brien, *Chem. Vap. Deposition* **1998**, *4*, 197.
[47] U. Patil, M. Winter, H.-W. Bexker, A. Devi, *J. Mater. Chem.* **2003**, *13*, 2177.
[48] W. A. Herrmann, N. W. Huber, O. Runte, *Angew. Chem. Int. Ed. Engl.* **1995**, *34*, 2187.
[49] P. A. Williams, J. L. Roberts, A. C. Jones, P. R. Chalker, J. F. Bickley, A. Steiner, H. O. Davies, T. J. Leedham, *J. Mater. Chem.* **2002**, *12*, 165.
[50] P. A. Williams, J. L. Roberts, A. C. Jones, P. R. Chalker, N. L. Tobin, J. F. Bickley, H. O. Davies, L. M. Smith, T. J. Leedham, *Chem. Vap. Deposition* **2002**, *8*, 163.
[51] S. Taylor, P. A. Williams, J. L. Roberts, A. C. Jones, P. R. Chalker, *Electron. Lett.* **2002**, *38*, 21.
[52] S. Horii, K. Yamamoto, M. Asai, H. Miya, M. Niwa, *Jpn. J. Appl. Phys., Part 1* **2003**, *42*, 5176.
[53] R. Matero, M. Ritala, M. Leskelä, A. C. Jones, P. A. Williams, J. F. Bickley, A. Steiner, T. J. Leedham, H. O. Davies, *J. Non-Cryst. Solids* **2002**, *303*, 24.
[54] K. A. Fleeting, P. O'Brien, A. C. Jones, D. J. Otway, A. J. P. White, D. J. Williams, *J. Chem. Soc., Dalton Trans.* **1999**, 2853.
[55] Y. F. Loo, R. O'Kane, A. C. Jones, H. C. Aspinall, R. J. Potter, P. R. Chalker, J. F. Bickley, S. Taylor, L. M. Smith, *J. Mater. Chem.* **2005**, *15*, 1896.
[56] Y. F. Loo, R. O'Kane, A. C. Jones, H. C. Aspinall, R. J. Potter, P. R. Chalker, J. F. Bickley, S. Taylor, L. M. Smith, *Chem. Vap. Deposition*, **2005**, *11*, 299.
[57] M.-Y. Ho, H. Gong, G. D. Wilk, B. W. Busch, M. L. Green, W. H. Lin, A. See, S. K. Lahiri, M. E. Loomans, P. I. Räisänen, T. Gutaffson, *Appl. Phys. Lett.* **2002**, *81*, 4218.
[58] R. B. Clark-Phelps, A. Srivasta, L. Cleveland, T. E. Seidel, O. Sneh, *Mater. Res. Soc. Symp. Proc.* **2001**, *670*, K2.21.
[59] P. A. Marshall, R. J. Potter, A. C. Jones, P. R. Chalker, S. Taylor, G. W. Critchlow, S. A. Rushworth, *Chem. Vap. Deposition* **2004**, *10*, 275.
[60] R. J. Potter, P. A. Marshall, P. R. Chalker, S. Taylor, A. C. Jones, T. C. Q. Noakes, P. Bailey, *Appl. Phys. Lett.* **2004**, *84*, 4119.
[61] M. Leskalä, M. Ritala, *J. Solid State Chem.* **2003**, *171*, 170.
[62] M. Hong, J. Kwo, A. R. Kortan, J. P. Mannaerts, A. M. Sergent, *Science* **1999**, *283*, 1897.
[63] Y. Shiokawa, R. Amano, A. Nomura, M. Yagi, *J. Radioanal. Nucl. Chem.* **1991**, *152*, 373.
[64] A. Weber, H. Suhr, *Mod. Phys. Lett.* **1989**, *B3*, 1001.
[65] R. L. Nigro, R. Toro, G. Malandrino, V. Raineri, I. L. Fragalà, *Electrochem. Soc. Proc.* **2003**, *2003-08*, 915.
[66] J. McAleese, J. C. Plakatouras, B. C. H. Steele, *Thin Solid Films* **1996**, *286*, 64.
[67] S. Chavalier, G. Bonnet, J. P. Larpin, *Appl. Surf. Sci.* **2000**, *167*, 125.
[68] N. L. Edleman, A. Wang, J. A. Belot, A. W. Metz, J. R. Babcock, A. M. Kawaoka, J. Ni, M. V. Metz, C. J. Flaschenreim, C. L. Stern, L. M. Liable-Sands, A. L. Rheingold, P. R. Markworth, R. P. H. Chang, M. P. Chudzik, C. R. Kanneworth, T. J. Marks, *Inorg. Chem.* **2002**, *41*, 5005.
[69] D. C. Bradley, J. S. Ghotra, F. A. Hart, *J. Chem. Soc., Dalton Trans.* **1973**, 1021.
[70] H. C. Aspinall, P. A. Williams, J. Gaskell, A. C. Jones, J. L. Roberts, L. M. Smith, P. R. Chalker, G. W. Critchlow, *Chem. Vap. Deposition* **2003**, *9*, 7.
[71] R. Anwander, F. C. Munck, T. Preiermeier, W. Scherer, O. Runte, W. A. Herrmann, *Inorg. Chem.* **1997**, *36*, 3545.
[72] P. A. Williams, A. C. Jones, H. C. Aspinall, J. M. Gaskell, P. R. Chalker, P. A. Marshall, Y. F. Loo, L. M. Smith, *Mat. Res. Soc. Symp. Proc.*, in press.
[73] H. C. Aspinall, J. Gaskell, P. A. Williams, A. C. Jones, P. R. Chalker, P. A. Marshall, L. M. Smith, G. W. Critchlow, *Chem. Vap. Deposition* **2004**, *10*, 13.
[74] H. C. Aspinall, J. Gaskell, P. A. Williams, A. C. Jones, P. R. Chalker, P. A. Marshall, L. M. Smith, G. W. Critchlow, *Chem. Vap. Deposition* **2004**, *10*, 83.
[75] H. C. Aspinall, J. Gaskell, P. A. Williams, A. C. Jones, P. R. Chalker, P. A. Marshall, J. F. Bickley, L. M. Smith, G. W. Critchlow, *Chem. Vap. Deposition* **2003**, *9*, 235.
[76] Y. F. Loo, R. J. Potter, A. C. Jones, H. C. Aspinall, J. M. Gaskell, P. R. Chalker, L. M. Smith, G. W. Critchlow, *Chem. Vap. Deposition* **2004**, *10*, 306.
[77] H. C. Aspinall, J. M. Gaskell, Y. F. Loo, A. C. Jones, P. R. Chalker, R. J. Potter, L. M. Smith, G. W. Critchlow, *Chem. Vap. Deposition* **2004**, *10*, 301.

[78] C. M. Carlson, J. C. Price, P. A. Parilla, D. S. Ginley, D. Niles, R. D. Blaugher, A. Goyal, M. Paranthaman, D. M. Kroeger, D. K. Christen, *Physica C* **1998**, *304*, 82.
[79] A. A. Molodyk, I. E. Korsakov, M. A. Novojilov, I. E. Graboy, A. R. Kaul, G. Wahl, *Chem. Vap. Deposition* **2000**, *6*, 133.
[80] S.-W. Kang, S.-W. Rhee, *J. Electrochem Soc.* **2002**, *149*, C345.
[81] M. Nieminen, M. Putkonen, L. Niinistö, *Appl. Surf. Sci.* **2001**, *174*, 155.
[82] K. Kukli, M. Ritala, V. Pore, M. Leskelä, T. Sajavaara, R. I. Hegde, D. C. Gilmer, P. J. Tobin, A. C. Jones, H. C. Aspinall, *Chem. Vap. Deposition* **2006**, *12*, 158.
[83] B. S. Lim, A. Rahtu, Pde Rouffignac, R. G. Gordon, *Appl. Phys. Lett.* **2004**, *84*, 3957.
[84] T. D. Manning, Y. F. Loo, A. C. Jones, H. C. Aspinall, P. R. Chalker, J. F. Bickley, L. M. Smith, G. W. Critchlow, *J. Mater. Chem.* **2005**, *15*, 3384.
[85] M. Ritala, M. Leskelä, *Appl. Surf Sci.* **1994**, *75*, 333.
[86] K. Kukli, K. Forsgren, J. Aarik, A. Aidla, T. Uutare, M. Ritala, A. Niskanan, M. Leskelä, A. Hårsta, *J. Cryst. Growth* **2001**, *231*, 262.
[87] M. Ritala, M. Leskelä, L. Niinistö, T. Prohaska, G. Friedbacher, M. Grasserbauer, *Thin Solid Films* **1994**, *250*, 72.
[88] J. Aarik, A. Aidla, A.-A. Kiisler, T. Uustare, V. Sammelselg, *Thin Solid Films* **1999**, *340*, 110.
[89] K. Forsgren, A. Hårsta, J. Aarik, A. Aidla, J. Westlinder, J. Olsson, *J. Electrochem. Soc.* **2002**, *149*, F139.
[90] M. Cho, J. Park, H. B. Park, C. S. Hwang, J. Jeong, K. S. Hyun, *Appl. Phys. Lett.* **2002**, *81*, 334.
[91] S. Codato, G. Corta, G. Rosetto, G. A. Rizzi, P. Zanella, P. Scard, M. Leoni, *Chem. Vap. Deposition* **1999**, *5*, 159.
[92] J. Niinistö, M. Putkonen, L.Niinistö, K. Kukli, M. Ritala, M. Leskelä, *J. Appl. Phys.* **2004**, *95*, 84.
[93] J. Niinistö, M. Putkonen, L. Niinistö, S. L. Stoll, K. Kukli, T. Sajavaara, M. Ritala, M. Leskelä, *J. Mater. Chem.* **2005**, *15*, 2271.
[94] D. M. Hausmann, E. Kim, J. Becker, R. G. Gordon, *Chem. Mater.* **2002**, *14*, 4350.
[95] K. Kukli, M. Ritala, M. Sajavaara, T. Keinonen, M. Leskelä, *Chem. Vap. Deposition* **2002**, *8*, 199.
[96] K. Kukli, M. Ritala, M. Leskelä, *Chem. Vap. Deposition*, **2000**, *6*, 297.
[97] A. C. Jones, P. A. Williams, J. L. Roberts, T. J. Leedham, H. O. Davies, R. Matero, M. Ritala, M. Leskelä, *Mater. Res. Soc. Symp. Proc.* **2002**, *716*, 145.
[98] K. Kukli, M. Ritala, M. Leskelä, T. Sajavaara, J. Keinonen, A. C. Jones, J. L. Roberts, *Chem. Mater.* **2003**, *15*, 1722.
[99] K. Kukli, M. Ritala, M. Leskelä, T. Sajavaara, J. Keinonen, A. C. Jones, J. L. Roberts, *Chem. Vap. Deposition* **2003**, *9*, 315.
[100] R. J. Potter, P. R. Chalker, T. D. Manning, H. C. Aspinall, Y. F. Loo, A. C. Jones, L. M. Smith, G. W. Critchlow, M. Schumacher, *Chem. Vap. Deposition* **2005**, *11*, 159.
[101] H. Seim, H. Mölsä, M. Nieminen, H. Fjellvåg, L. Niinisto, *J. Mater. Chem.* **1997**, *7*, 449.
[102] J. Päiväsaari, M. Putkonen, L. Niinisto, *Thin Solid Films* **2004**, *472*, 275.
[103] B. S. Lim, A. Rahtu, J.-S. Park, R. G. Gordon, *Inorg. Chem.* **2003**, *42*, 7951.
[104] B. S. Lim, A. Rahtu, R. G. Gordon, *Nat. Mater.* **2003**, *2*, 749.
[105] J. Niinistö, M. Putkonen, M. Ritala, P. Raisanen, A. Niskanen, M. Leskelä, *US Patent 6 858 546* **2005**.
[106] K. Kukli, M. Ritala, T. Pilvi, T. Sajavaara, M. Leskelä, A. C. Jones, H. C. Aspinall, D. C. Gilmer, P. J. Tobin, *Chem. Mater.* **2004**, *16*, 5162.
[107] M. A. Cameron, S. M. George, *Thin Solid Films* **1999**, *348*, 90.
[108] R. Matero, M. Ritala, M. Leskelä, T. Sajavaara, A. C. Jones, J. L. Roberts, *Chem. Mater.* **2004**, *16*, 5630.
[109] V. Pore, A. Rahtu, M. Leskelä, M. Ritala, T. Sajavaara, J. Keinonen, *Chem. Vap. Deposition* **2004**, *10*, 143.
[110] K. Kukli, M. Ritala, M. Leskelä, *J. Electrochem. Soc.* **1995**, *142*,1670.
[111] K. Kukli, M. Ritala, M. Leskelä, T. Sajavaara, J. Keinonen, A. C. Jones, N. L. Tobin, *Chem. Vap. Deposition* **2004**, *10*, 91.

